# Genetic Algorithm-Based Uncoded M-ary Phase Shift Keying Space-Time Labelling Diversity with Three Transmit Antennas for Future Wireless Networks

Shaheen Solwa
*EECE Department*
*University of KwaZulu-Natal*
Durban, South Africa
shaheensolwa786@gmail.com

Mohamed K. Elmezughi
*EECE Department*
*University of KwaZulu-Natal*
Durban, South Africa
m.k.elmezughi@gmail.com

Ayodeji James Bamisaye
*EECE Department*
*University of KwaZulu-Natal*
Durban, South Africa
ayobamisaye@gmail.com

Dauda Ayanda
*EECE Department*
*University of KwaZulu-Natal*
Durban, South Africa
d.ayanda@ieee.org

Ali Almaktoof
*ECE Department*
*Cape Peninsula University of Technology*
Cape Town, South Africa
almaktoofa@cput.ac.za

M. T. E. Kahn
*ECE Department*
*Cape Peninsula University of Technology*
Cape Town, South Africa
khant@cput.ac.za

***Abstract*—Recently, the three transmit uncoded space-time labelling diversity (USTLD) system was introduced in literature for quadrature amplitude modulation (QAM) and amplitude phase shift keying (APSK) schemes. However, the new scheme had not been applied to the phase shift keying (PSK) modulation technique. Due to the structure of M-PSK constellations, existing third mapper symmetry-based heuristics could not produce mapper designs. In this paper, a genetic algorithm (GA) is proposed to produce the third mapper design for three transmit USTLD PSK systems. The three transmit antennas USTLD M-PSK scheme is simulated in the fast-fading channel where M is the order of modulation. Numerical analysis show that the analytical results are validated by Monte Carlo simulations with a tight match at high SNR. At a bit error rate(BER) of $10^{-6}$, the 8PSK and 32PSK schemes exhibit gains of $\approx 2\ dB$ and $\approx 8\ dB$ while at the BER of $10^{-5}$, the 16PSK and 64PSK schemes exhibit a gain of $\approx 4\ dB$ and $\approx 5\ dB$, respectively.**

***Keywords— Genetic algorithm, USTLD, M-PSK, QAM, labeling diversity, heuristics, wireless communications.***

## I. Introduction

The forth-generation (4G) wireless communication standards such as WiMAX and LTE have already adopted a MIMO structure as an integral part of the air interface specifications [1]. By employing multiple antennas at both the transmitter and receiver, additional diversity, multiplexing, array gain, enhanced channel capability is achieved, and fewer errors are detected during transmission. Recently, there has been an influx of literature on error performance analysis of MIMO-STBC systems with some sort of receiver diversity [2], [3].

The demand for high data rate wireless communications is growing at an exponential rate which requires systems to more efficient and reliable. To achieve reliable high data rate communications, space-time block coded (STBC)-based multiple-input multiple output (MIMO) systems are employed [4]. The power of STBCs lie in the usage of multiple received versions of the same signal to mitigate the impairments of wireless multipath fading channels. In order to improve the bandwidth efficiency of MIMO-STBC systems, many techniques have been investigated in [5]-[7]. In [5], the authors extend signals to the spatial domain, but limited the system to the number of transmit antenna that can be used to achieve high bandwidth efficiencies.

Uncoded Space-Time Labelling Diversity (USTLD) is a recent innovative scheme proposed as a direct extension over the Alamouti STBC [8]. USTLD improves error performance in STBC systems by employing a Multiple-Input Multiple-Output (MIMO) structure and implementing Labelling Diversity (LD). In USTLD, LD is achieved by using symbol pairs from different binary mappings to encode information codewords. To transmit a single codeword using an M-ary constellation, there exists M possible symbol pairs that can be transmitted over different time slots. But, the receiver can detect $M^2$ number of symbol pairs. Since only $M$ of the $M^2$ possible symbol pairs are valid, error performance is improved [8]. The level of which LD is achieved depends on the constellation assignment of the binary mappers employed. The aim of LD mapper design is to position adjacent symbols on each constellation further apart than in the base constellation [9]. [9] suggests a design metric to evaluate these mappers as well as design techniques that can be used to design LD mappers.

Recently, Ayanda *et al.* [10] designed a three transmit USTLD system based on the two transmit USTLD system. The proposed system used three binary mappings that used existing mappers for secondary constellations and proposed a new heuristic transform to design the third mapper. The authors suggest readers to refer to [11] for a detailed study of the heuristic transform. Ayanda *et al.* [10] applied this system to M-QAM and M-APSK constellations due to symmetry [10]. This heuristic transform cannot be applied to M-PSK constellations due to its number of plot points. Hence, this prompted studies into applying other existing techniques to design third mappers for three transmit USTLD with M-PSK modulation.

A very innovative approach to designing LD mappers had been proposed by [9] in the form of a Genetic Algorithm. A Genetic Algorithm (GA) is a meta-heuristic algorithm that mimics the process of evolution and natural selection [9]. GAs solve complex combinatorial problems in an iterative manner. In this paper, we focus on designing third mappers for M-PSK constellations for three transmit USTLD systems using a multi-function optimization GA.

### A. Motivation and Contributions

The PSK modulation scheme is widely adopted within the area of radio communication systems, particularly well-suited for the data communications area [12]. Recently, the adaption of the MIMO USTLD scheme for radio communications using the PSK transmission model had been introduced for two transmit USTLD systems [11]. Motivated to improve on the literature mentioned, the main aim of this study is to adapt the work carried out in [11], [10] and apply it to the M-PSK modulation. Furthermore, the study also looks to improve the link reliability of radio communications in the presence of noise and a multipath fading channel compared to the existing two-transmit USTLD M-PSK scheme. The contributions of the paper are stated as follows:

- Heuristic algorithms for designing the third optimized mapper cannot be used due to the PSK constellation structure. Hence, a Multi-Function Optimization genetic algorithm is designed to develop tertiary M-PSK mappers.
- The error performance of the Three Transmit M-PSK USTLD scheme is compared to the existing two-transmit USTLD M-PSK scheme using rate one.

### B. Structure and Notation

The remainder of this paper is structured as follows: Section 2 summarizes the system model of the three transmit USTLD system. Included in Section 2 is an analytical expression for the three transmit USTLD and a suggested expression to design third mappers. Section 3 describes the Genetic Algorithm used in this paper to design the third mappers. Section 4 presents the results of the paper. Concluding remarks are discussed in Section 5.

In terms of notation, scalars and vectors are in boldface and italics respectively. $\|\cdot\|$ represents the Frobenius norm of a vector, $|\cdot|$ represents the absolute value of a scalar and $(\cdot)!$ represents the factorial of a scalar.

## II. SYSTEM MODEL

In this paper, a USTLD MIMO-structured system with $N_T = 3$ transmit antenna and $N_R$ receive antenna are considered. USTLD systems use constellations of binary mappings to encode information to be transmitted. Consider an n-bit information codeword, $D$ which are fed into mappers $\Omega_1, \Omega_2$ and $\Omega_3$ which produces the symbols $\Omega_1(D)$, $\Omega_2(D)$ and $\Omega_3(D)$ respectively. These symbols are transmitted over three time slots. Mapper $\Omega_t$ is used to encode information in the t-th time slot, where $t - th, t \epsilon [1:3]$ ,. Therefore, the received vector, $\boldsymbol{y}_t$ , of size $N_R \, x \, 1$ in time slot **t** is represented by:

$$\boldsymbol{y}_t = \sqrt{\frac{\rho}{3}}\left[\boldsymbol{h}_{t,1}\,\Omega_t\left(D_{(1)}\right) + \boldsymbol{h}_{t,2}\,\Omega_t\left(D_{(2)}\right) + \boldsymbol{h}_{t,3}\,\Omega_t(D_{(3)})\right] + \boldsymbol{n}_t, \quad (1)$$

where $\rho$ is the average signal-to-noise ratio at each receiver and $\boldsymbol{n}_t$ is the $N_R \, x \, 1$ additive white Gaussian noise (AWGN) vector. $\boldsymbol{h}_{t,u}, t, u \, \epsilon \, [1:3]$ is the $N_R \, x \, 1$ vector that represents the multipath fading that the symbol experiences due to transmission from antenna $u$ in time slot $t$. The fading is assumed to be frequency flat and follow the Rayleigh distribution with zero mean and unit variance. Fading can either be of quasi-static or fast fading nature over the three time slots. Both noise and fading phase distributions are assumed to be uniform.

At the receiver, maximum likelihood (ML) detection algorithm is used to estimate the transmitted information symbols. We assume perfect channel state information is available at the receiver. Hence, the ML detection scheme can be formulated as:

$$\widehat{D_{(1)}}, \widehat{D_{(2)}}, \widehat{D_{(3)}} = arg \min_{D_{(1)}, D_{(2)}, D_{(3)}} \left\| \boldsymbol{y}_l - \sum_{u=1}^{3} \sqrt{\frac{\rho}{3}}\, \boldsymbol{h}_{t,u}\,\Omega_t\left(\widehat{D_{(u)}}\right)\right\|^2, t \, \epsilon \, [1:3], \quad (2)$$

where $\widehat{D_{(1)}}, \widehat{D_{(2)}}, \widehat{D_{(3)}}$ are the estimated symbols that are detected at the receiver and $D_{(u)}$ represents the transmitted symbols over the three time slots respectively.

## III. ANALYTICAL ERROR PERFORMANCE OF USTLD SYSTEMS WITH THREE TRANSMIT ANTENNAS

From the model outlined in section 2, the Average Bit Error Probability for the three-transmit USTLD system was derived in [10]. The final expression was given as:

$$ABEP(\rho) = \frac{1}{Mr} \sum_{D=0}^{M-1} \sum_{\substack{\widehat{D}=0 \\ \widehat{D} \neq D}}^{M-1} \mathrm{N}(D, \widehat{D}) \mathrm{P}(\mathrm{D} \rightarrow \widehat{\mathrm{D}}), \quad (3)$$

where $M$ is the order of modulation, $r = \log_2 M$ is the number of bits per symbol on the constellation and $\mathrm{N}(D, \widehat{D})$ is the number of bit errors between transmitted and estimated symbols respectively. $\mathrm{P}(\mathrm{D} \rightarrow \widehat{\mathrm{D}})$ is the pairwise error probability (PEP) that assumes two triads of transmitted symbols are detected correctly while one triad of symbols is detected with error.

From [10], the resulting PEP can be stated as:

$$P(D \rightarrow \widehat{D}) = \frac{1}{4n}\prod_{t=1}^{3}(1+\frac{\rho d_t^2}{12})^{-N_R} + \frac{1}{2n}\sum_{s=1}^{n}\prod_{t=1}^{3}(1+\frac{\rho d_t^2}{12\sin^2(\frac{s\pi}{2n})})^{-N_R}, \quad (4)$$

where $n$ is a relatively large integer $n > 10$ and $d_t = |\Omega_t(D) - \Omega_t(\widehat{D})|, t \in [1:3]$ is the Euclidean distance between the points $D$ and $\widehat{D}$ on the constellation of $\Omega_t$. A detailed derivation of (4) can be found in section 3 in [10]. At high SNR -$\frac{\rho d_t^2}{12} \gg 1, t \in [1:3]$, [11] shows that the PEP can be reduced to the following equation:

$$P(L \rightarrow \hat{L}) = \frac{1}{4n}(\frac{\rho d_1^2}{12}\frac{\rho d_2^2}{12}\frac{\rho d_3^2}{12})^{-N_R} + \frac{1}{2n}\sum_{s=1}^{n}(\frac{\rho d_1^2}{12\sin^2(\frac{s\pi}{2n})}\frac{\rho d_2^2}{12\sin^2(\frac{s\pi}{2n})}\frac{\rho d_3^2}{12\sin^2(\frac{s\pi}{2n})})^{-N_R}. \quad (5)$$

## IV. DESIGN AND OPTIMIZATION OF SECONDARY AND TERTIARY LABELLING DIVERSITY MAPPERS

From (5), it can be seen that USTLD systems are dependent on the minimum product Euclidean distance $d_1 d_2 d_3$. By maximising the minimum product distance, we minimize the error performance of the USTLD system. In this case, it is achieved by employing three mapper designs for the USTLD system. The resultant optimization formula can be stated as:

$$\beta(\Omega_1^M, \Omega_2^M) = \underset{\substack{L,\hat{L} \in [0:M-1] \\ L \neq \hat{L}}}{\operatorname{argmin}} \prod_{t=1}^{2} d_t, \quad (6)$$

$$\beta(\Omega_2^M, \Omega_3^M) = \underset{\substack{L,\hat{L} \in [0:M-1] \\ L \neq \hat{L}}}{\operatorname{argmin}} \prod_{t=1}^{3} d_t. \quad (7)$$

Research efforts such as in [8], [9], [11], [13] have been prioritised on maximising the minimum product distance between symbols on an M-ary constellation, where M is the order of modulation. From Samra and Krasicki [15], [16], an instance of the QAP is used to solve for these optimal mapper designs. However, this approach is too computationally expensive ($M!$ and $M^5$) and is limited to 16-ary optimal constellations only. Seddik [14] introduced a heuristic algorithm which produced a mapper design that rearranged the rows and columns of the source constellation such that any two adjacent rows or columns are nonadjacent. Xu *et al.* [8] proposed a heuristic design which swapped diagonal pairs to produce a mapper design.

For this paper, the authors use – to the best of the authors knowledge – the most optimal mapper designs found in [15] as secondary mappers. Recently, [9] designed a Genetic algorithm to produce close to optimal mapper designs for two transmit systems. For this paper, the Genetic Algorithm will be used to design the third mapper for the M-PSK constellations, where $M = 8, 16, 32, 64$. The description of the Genetic Algorithm is given in the next section. The heuristic design for the third mapper presented in [18], [19] could not be used as it has an odd number of terms to be transformed.

## V. MAPPER DESIGN

### A. Genetic Algorithm

Existing mapper design techniques used to produce tertiary mapper designs for three transmit antennas USTLD systems are limited to the following constraints: i) algorithmic approaches are too computationally expensive [15] and ii) the heuristic-based approach relies on symmetry. M-PSK constellation points are not placed in a symmetric orientation, hence the heuristic approach cannot be applied to produce tertiary mapper designs. To combat the limitations, a multi-function genetic algorithm (GA) is proposed to produce tertiary mapper designs for three transmit antennas USTLD systems. The GA is described below.

### B. Logic of Genetic Algorithm

Since the GA is a multi-function optimization algorithm, it does not follow the one step logic, but a looped logic. The GA will first initiate the population to solve for the secondary mapper using the biological-inspired ‘mating’ process of crossover and mutation. Once the GA has found a solution to the secondary mapper design, the chromosomes in the population is used as the initial population used to design the tertiary mapper. The next subsections describe the entire process of the GA in more detail.

### C. Encoding of Chromosomes

Candidate solutions for a Genetic Algorithm are represented as a chromosome, $\delta$. Information encoded within chromosomes are known as ‘genes’, represented as $\alpha_i$, where $i \in [0: M-1]$. Each ‘gene’ contains a label associated with a point on the M-ary constellation. Thus, a chromosome can be defined as:

$$\delta = [\alpha_0, \alpha_1, \dots, \alpha_{M-1}]. \quad (8)$$

### D. Initial Population

A population, $\boldsymbol{P}$, represents a set of $p$ chromosomes. The initial population, $\boldsymbol{P}^{(0)}$, contains a set of unique permutations of the chromosome. If exhaustive search or heuristic mapper designs are available, these are encoded as chromosomes and added to the initial population of the Genetic Algorithm. This ensures that the Genetic Algorithm will either match or improve upon existing mapper designs. A population $\boldsymbol{P}$ can be defined as:

$$\boldsymbol{P} = [\delta_0, \delta_1, \dots, \delta_{\boldsymbol{P}-1}]. \quad (9)$$

### E. Crossover Operator

The crossover operator is the most influential function within the GA. Crossover is essentially used to produce offspring chromosome that gain the desirable properties of parent chromosomes. In recent literature, [9] proposed a new crossover technique purely for designing LD mappers, termed the K-Hypersphere Swap crossover (K-HSX). The technique was proposed for the USTLD scheme with two transmit antennas. Two parent biological crossover techniques had been investigated in [17] to further improve upon the ability of the

GA to produce closer-to-optimal LD mapper designs. The single-point, multi-point and ordered crossover techniques were investigated. The techniques investigated produced mapper designs that matched or improved upon those produced by the GA in [9].

Hence for the application of this GA, the Single Point Crossover was chosen for implementation. From literature, the Single Point Crossover is the most approved crossover that is widely in use. The methodology of the Single Point Crossover is as follows: i) A crossover point is selected randomly along the string of the first parent chromosome. The same occurs for the second parent chromosome. This creates a head and tail for each parent chromosome, ii) the tails of each parent chromosome are swapped, hence creating two offspring chromosomes. Fig. 1 is shown for clarity purposes.

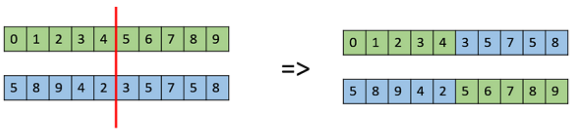


Fig. 1. The single point crossover technique.

### *F. Mutation Operator*

Mutation is a probabilistic event that occurs after crossover. Mutation is a genetic operator used to maintain genetic diversity in offspring chromosomes. Mutation is the 'exploration' stage of the GA process. Mutation was observed to be the most important factor for the convergence of the GA. In the context of this GA, mutation will occur if two randomly selected genes within an offspring chromosome is swapped. For the application of this GA, the probability of mutation occurring is $P_m$. Fig. 2 represents an illustration of the mutation operator.

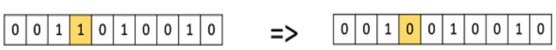


Fig. 2. Illustration of the mutation operator.

### *G. Chromosome Filter*

The GA designed has to satisfy a single constrain for designing LD mappers that all genes should be unique in a chromosome. Hence, due to the nature of the single point crossover, a filter was employed to remove 'illegal' chromosomes in the population after crossover. The filter will remove all chromosomes with duplicate genes and keep all chromosomes with unique genes respectively.

### *H. Evaluation of Chromosomes*

After 'mating' (crossover and mutation), natural selection of chromosomes is imitated. Parent and offspring chromosomes are added back into the population and evaluated according to a fitness function. These functions are given as (6) and (7). The best **p** number of chromosomes are selected and make up the next generations population, $\boldsymbol{P}^{(i+1)}$. The authors remind the readers that for the first stage of the GA, $\Omega_1$ is known to solve for $\Omega_2$, while during the second stage, $\Omega_2$ is known to solve for $\Omega_3$.

### *I. Termination of Genetic Algorithm*

Termination of a Genetic Algorithm occurs in one of two cases:

- Maximum number of iterations have been reached
- Convergence of a population

For the first case, if the Genetic Algorithm terminates at the maximum number of iterations, no optimal, stable or convergent solutions are found, hence the chromosome with the highest fitness is chosen as the best possible solution and is regarded as a sub-stable solution. In the second case, all chromosomes in the population have converged to a single fitness value, $\delta(\Omega_2, \varphi_a) = \delta(\Omega_2, \varphi_b), \forall\, \varphi_a, \varphi_b \in \mathrm{P}$ and $\delta(\Omega_3, \varphi_a) = \delta(\Omega_3, \varphi_b), \forall\, \varphi_a, \varphi_b$. The solutions produced by the Genetic Algorithm is then said to be either stable or locally/ globally optimal. The Genetic Algorithm is constrained to $n_{max}$ number of iterations.

Termination for this GA occurs twice, namely, i) After the convergence of the GA that solves for $\Omega_2$ and ii) After the convergence of the GA that solves for $\Omega_3$.

## VI. RESULTS AND DISCUSSIONS

### *A. Validation of Analytical Results in the Fast-Fading Channel*

The results presented in this section are for the analytical expression in (3) and the Monte Carlo simulations are shown in Fig. 3 for the fast-fading channel respectively. The modulation orders are 8-PSK, 16-PSK, 32-PSK and 64-PSK. In Fig. 3, the analytical results closely matched the Monte Carlo simulation results in the fast-fading channel.

The GA had produced optimal mappers for the 8PSK, 16PSK, 32PSK and 64PSK constellations for the three transmit antennas USTLD scheme. The output of the GA is summarized in table 1.

TABLE I. THE LD VALUES ACHIEVED BY MAPPER $\Omega_2^M$ AND $\Omega_3^M$

| Modulation | $\boldsymbol{\beta(\Omega_1^M, \Omega_2^M)}$ | $\boldsymbol{\beta(\Omega_2^M, \Omega_3^M)}$ |
|---|---|---|
| 8PSK | 1.4140 | 1.0820 |
| 16PSK | 0.5857 | 0.2286 |
| 32PSK | 0.2178 | 0.1734 |
| 64PSK | 0.0575 | 0.0320 |

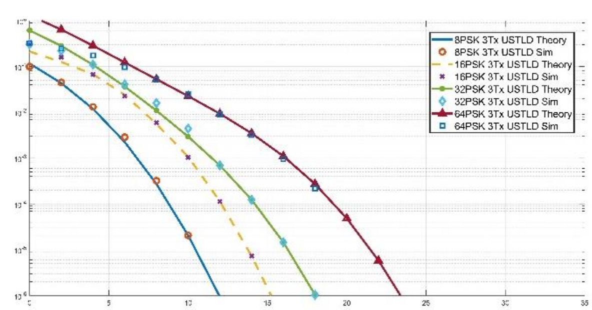


Fig. 3. BER Curves of the Three-Transmit USTLD with M-PSK scheme in the fast-fading channel.

### B. *BER Comparison between M-PSK USTLD with $N_T = 3$ and M-PSK USTLD with $N_T = 2$*

In this section, the three-transmit USTLD M-PSK scheme is compared to the existing two-transmit USTLD M-PSK scheme. For simplicity, Fig. 4 illustrates the error performance comparison between the 8PSK and 32PSK schemes, while Fig. 5 illustrates the error performance comparison between the 16PSK and 64PSK schemes respectively. For the USTLD 8PSK scheme, the three-transmit USTLD 8PSK scheme exhibits a $\approx 2dB$ gain over the two-transmit USTLD scheme while the three-transmit USTLD 32PSK scheme exhibited a gain of $\approx 8dB$ over the two-transmit USTLD 32PSK scheme respectively at a BER of $10^{-6}$. The three-transmit USTLD 16PSK scheme was shown to have a gain of $\approx 4dB$ over the two-transmit USTLD 16PSK scheme. Finally, the three-transmit USTLD 64PSK scheme had exhibited a $\approx 5dB$ gain over the two-transmit USTLD 64PSK scheme respectively. Finally, it can be confirmed that as more antennas are introduced into the USTLD system and close-to-optimal secondary and tertiary LD mappers are designed, the BER can be improved. The research findings of this work are valuable for achieving reliable wireless communication systems capable of meeting future needs. These requirements are the primary motivation for accelerating the research toward accurate and high-speed communication networks [20]-[25].

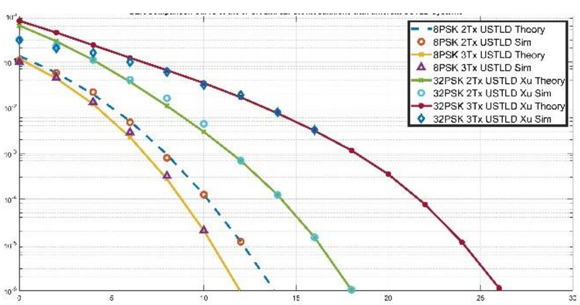


Fig. 4. Comparison between Two-Transmit and Three-Transmit USTLD M-PSK schemes with M = 8 and 32

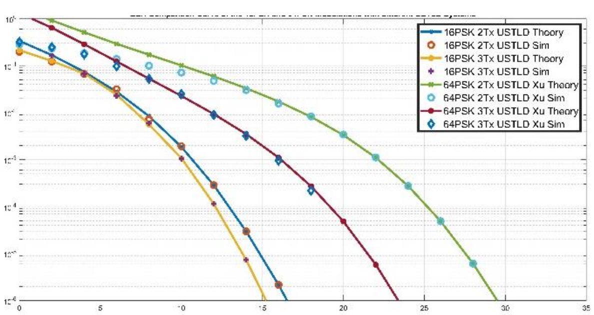


Fig. 5. Comparison between Two-Transmit and Three-Transmit USTLD M-PSK schemes with M = 16 and 64.

## VII. CONCLUSION

Three transmit antennas USTLD systems have been recently proposed to improve the error performance by increasing antenna diversity. However, due to its structure, the heuristic algorithm designed for developing the third mapper could not be applied to M-PSK constellations. The GA is implemented to design close-to-optimal second and third mapper designs to mitigate this limitation. As a result, the GA was able to produce mapper designs without constraint. The three transmit USTLD M-PSK scheme was simulated in the fast-fading channel. Monte Carlo simulations demonstrated a close fit with the analytical results. The proposed 8PSK and 32PSK three transmit antennas USTLD schemes had illustrated gains of $2\,dB$ and $8\,dB$ compared to the existing two transmit antennas USTLD M-PSK scheme at the BER of $10^{-5}$. The 16PSK and 64PSK schemes demonstrated gains of $4\,dB$ and $5\,dB$ at a BER of $10^{-5}$ over the two transmit USTLD M-PSK schemes.

## REFERENCES

[1] G. Maiti and A. Chandra, "Performance of Alamouti coded MIMO systems with switch and examine combining," *IEEE Symposium Comput. Informatics*, pp764 – 769, Mar. 2011.

[2] W. Lo and N. C. Beaulieu, "Effects of channel errors on receiver selection-combining schemes for Alamouti MIMO systems with BPSK," *IEEE Trans. Commun*.,vol. 54, no. 1, pp. 169-178, Jan. 2006.

[3] Z. Chen, J. Yuan, and B. Vucetic, "Analysis of transmit antenna selection/maximal-ratio combining in Rayleigh fading channels," *IEEE Trans. Veh. Tech.*, vol. 54, no. 4, pp. 1312-1321, Jul. 2005.

[4] Dlodlo, B. Xu, H and Pillay, N. "Bandwidth Efficiency Improvement for Differential Alamouti Space-Time Block Codes Using M-QAM", *SAIEE Africa Res. J.*, vol. 109, no. 4, pp. 217-222, Dec. 2018.

[5] E. Basar, U. Aygolu, E. Panayirci and H. V. Poor: "Space-time block coded spatial modulation", *IEEE Trans. Commun.*, vol. 59, No. 3, pp. 823-832, Mar. 2011.

[6] H. Lee, M. Siti, W. Zhu and M. Fitz: "Super-orthogonal space-time block code using a unitary expansion," *IEEE 60th Annual Conf. Vehicular Tech., Los Angeles*, pp. 2513-2517, Sep. 2004.

[7] Z. A. Baloch, M. U. Baloch and N. Hussain: "Efficiency improvement of space time block codes", *Int. J. Commun., Netw. and Syst. Sci*., vol. 3, no. 6, p. 507-510, Jun. 2010.

[8] H. Xu, K. Govindasamy and N. Pillay, "Uncoded space-time labeling diversity," *IEEE Commun. Lett.*, vol. 20, no. 6, pp 1511 – 1514, Jun. 2016.

[9] S. S. Patel, T. Quazi and H. Xu, "A genetic algorithm for designing uncoded space-time labelling diversity mappers," *IEEE Int. Workshop on Sig. Proc. Syst. (SiPS)*, pp 1 – 6, Oct. 2018.

[10] D. O. Ayanda, "Performance analysis of M-ary amplitude and phase shift keying uncoded space-time labeling diversity with three transmit antennas in nonlinear Rician channels," Trans. Emer. Telecomm. Tech. , vol. 32, no. 11, Nov. 2021.

[11] D. O. Ayanda, H. Xu and N. Pillay, "Uncoded M-ary quadrature amplitude modulation space-time labeling diversity with three transmit antennas," Int. Journ. Commun. Syst. vol. 31, no. 18, Dec. 2018.

[12] K. S. Faraj and S. Fidawi. (2020). Phase Shift Keying (PSK). doi:10.13140/RG.2.2.22811.90409.

[13] M. Krasicki, "Improved labelling diversity for iteratively-decoded multi-antenna systems," *7th Int. Wirel. Commun. and Mobi. Comput. Conf.*, pp 356 - 364, Jul. 2011.

[14] K. G. Seddik, A. S. Ibrahim and K. J. Liu, "Trans-modulation in wireless relay networks," *IEEE Trans. Commun. Lett.*, vol. 12, no. 3, pp 170 – 172, Mar. 2008.

[15] H. Samra, Z. Ding and P. Hahn, "Symbol mapping diversity design for multiple packet transmission," *IEEE Trans Commun.*, vol. 53, no. 5, pp 810 – 817, May 2005.

[16] M. Krasicki, "Essence of 16-QAM labelling diversity," *Elect. Lett.*, vol. 49, no. 8, pp 567 – 569, Jun. 2013.

[17] S. Solwa, "A performance study of a genetic algorithm based mapper design for uncoded space-time labeling diversity. ," *Trans. Emer. Telecomm. Tech.*, under view.

[18] Y. Huang and J. A. Ritcey, "Optimal constellation labelling for iteratively decoded bit-interleaved space-time coded modulation.," *IEEE Trans. Inf. Theory*, vol 51, no. 5, pp 1865 – 1871, Apr. 2005.

[19] S. Ejaz, F. Yang and H. Xu, "Labelling diversity for 2x2 WLAN coded networks," *Radio Eng.*, vol. 24, no. 9, pp 695 – 697, 2015.

[20] M. K. Elmezughi and T. J. Afullo, "An Efficient Approach of Improving Path Loss Models for Future Mobile Networks in Enclosed Indoor Environments," *IEEE Access*, vol. 9, pp. 110332–110345, Aug. 2021.

[21] M. K. Elmezughi, T. J. Afullo, and N. O. Oyie, "Investigating the Impact of Antenna Heights on Path Loss Models in an Indoor Corridor Environment," *icABCD2020. Conf., IEEE*, Sep. 2020, pp. 1–7.

[22] T. S. Rappaport, G. R. Maccartney, M. K. Samimi, and S. Sun, "Wideband Millimeter-Wave Propagation Measurements and Channel Models for Future Wireless Communication System Design," *IEEE Trans. Commun.*, vol. 63, no. 9, pp. 3029-3056, Sep. 2015.

[23] M. K. Elmezughi and T. J. Afullo, "Evaluation of Line-of-Sight Probability Models for Enclosed Indoor Environments at 14 to 22 GHz," *icABCD2021. Conf., IEEE*, Sep. 2021, pp. 1–7.

[24] T. S. Rappaport, S. Sun, R. Mayzus, H. Zhao, Y. Azar, K. Wang, G. N. Wong, J. K. Schulz, M. Samimi, and F. Gutierrez, "Millimeter Wave Mobile Communications for 5G Cellular: It will Work!" *IEEE Access*, vol. 1, pp. 335-349, 2013.

[25] M. K. Elrnezughi, T. J. Afullo, and N. O. Oyie, "Performance study of path loss models at 14, 18, and 22 GHz in an indoor corridor environment for wireless communications," *SAIEE Afr. Res. J.*, vol. 112, pp. 32-45, Mar. 2021.